

Reconstruction of the Adaptable Deployable Entry and Placement Technology Sounding Rocket One Flight Test

Jake A. Tynis*, Christopher D. Karlgaard† and Joseph D. Williams‡
Analytical Mechanics Associates Inc., Hampton, VA, 23666, USA

Soumyo Dutta §
NASA Langley Research Center, Hampton, VA 23681, USA

The Adaptable Deployable Entry and Placement Technology Sounding Rocket One flight test is a demonstration experiment for deployable atmospheric decelerator technologies. The suborbital flight test occurred on 12 September 2018, at the White Sands Missile Range. Data from on-board and ground-based sensors were collected, from which the as-flown trajectory was reconstructed using an iterative extended Kalman filter-smoother. This paper describes the methodology, test vehicle instrumentation, and data analysis results from the flight test trajectory reconstruction.

I. Introduction

THE Adaptable Deployable Entry and Placement Technology (ADEPT) Sounding Rocket One (SR-1) flight test was the first high altitude flight of a novel deployable fabric decelerator system. This demonstration program tested new and enabling decelerator technologies for future atmospheric missions. This mission architecture enables large heatshield surface areas to fit within launch vehicle stowed volume requirements. Specifically, the ADEPT SR-1 mission tested a 0.7 meter deployable heat shield from a sounding rocket launch vehicle. Figure 1 provides an overview of the ADEPT SR-1 mission concept of operations.

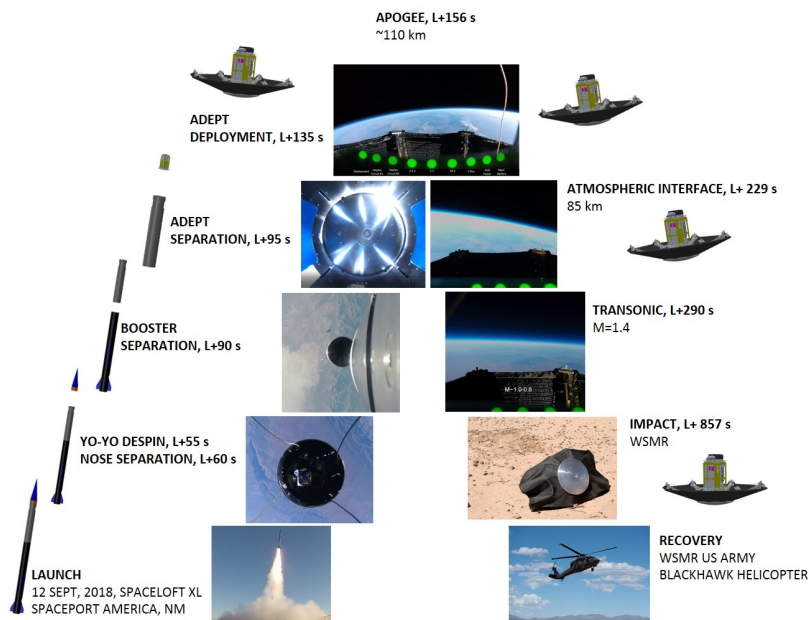


Fig. 1 ADEPT SR-1 Concept of Operations.

*Aerospace Engineer, Member AIAA

†Supervising Engineer, Senior Member AIAA

‡Systems Engineer

§Aerospace Engineer, Atmospheric Flight and Entry Systems Branch, 1 N. Dryden St., M/S 489, and Member AIAA.

The ADEPT SR-1 flight vehicle was designed as a technology demonstrator utilizing a 3-unit CubeSat chassis as the primary structure. The 11 kg vehicle was stowed within the payload canister of the sounding rocket and separated from the launch vehicle after booster burnout and despin. Avionics, including sensors, C-band transponder, and heatshield deployment equipment were entirely contained within the ADEPT SR-1 vehicle and required no interaction with the launch vehicle. The fabric heatshield was mechanically deployed at a predetermined mission time after separation from the launch vehicle.

The ADEPT SR-1 flight test was successfully launched from Spaceport America on 12 September 2018. The vehicle was successfully released from the sounding rocket approximately 96 seconds after launch. The vehicle reentered the atmosphere and impacted approximately 857 seconds after launch within the boundaries of the White Sands Missile Range. This paper details the reconstruction of the vehicle performance utilizing available data collected during the flight test.

II. Trajectory Reconstruction Methodology

A. NewSTEP

The reconstructed ADEPT SR-1 trajectory was computed by a MATLAB-based Iterative Extended Kalman Filter-Smoother code known as the New Statistical Trajectory Estimation Program (NewSTEP) [1, 2]. This software is a modernized and generalized implementation based on the legacy Statistical Trajectory Estimation Program (STEP) [3], which was developed during the 1960's. NewSTEP has the capability to process many types of sensor measurements to produce an optimal estimate of the as-flown vehicle trajectory, including various types of onboard sensors such as Inertial Measurement Unit (IMU), Global Positioning System (GPS), air-data sensors, and ground-based measurements such as radar.

For ADEPT SR-1, NewSTEP was configured to process three separate onboard IMU measurements, GPS data, atmospheric weather balloon measurements, and ground-based radar tracking data. The reconstruction process was tested extensively prior to the ADEPT SR-1 launch by making use of simulated sensor data sets created by the Program to Optimize Simulated Trajectories II (POST2) [3, 4].

III. Flight Test Instrumentation & Sensors

A. ADEPT SR-1 Sensor Description

The reconstruction fidelity and accuracy of the ADEPT SR-1 flight vehicle performance was dependent on the availability of instrumentation and sensor data post flight. A combination of onboard sensors, external measurements, and other data sources were identified preflight for the reconstruction process. An instrumentation and sensor product availability matrix was established to determine the minimum success criteria and quality for a post flight reconstruction. A description of data products and general proposed usage are included in Table 1.

Table 1 ADEPT SR-1 Data Sources.

Sensor Type	Measurement Device	Notes
IMU	Affordable Vehicle Avionics (AVA)	Critical for Orientation
IMU	Next Generation IMU (NGIMU)	Critical for Orientation
IMU	Memsense H3	Critical for Launch Vehicle Orientation
Tracking Radar	C-Band Transponder / Radar	Position & Velocity Data
GPS	AVA	Position & Velocity Data
GPS	Autonomous Flight Termination Unit (AFTU) A/B	Position & Velocity Data
Magnetometer	AVA	Orientation
Magnetometer	NGIMU	Orientation

The critical data product for reconstruction of the SR-1 trajectory was data from an IMU. This was the only instrument that collected acceleration and angular data at a resolution sufficient for orientation determination throughout

the flight test. Therefore, the minimum criteria for successful orientation reconstruction was data from at least one IMU. The minimum success criteria for reconstruction of position and velocity was determined to be a tracking radar only data product. Tracking radar does not generate an orientation history but can provide qualitative data regarding the overall performance of the vehicle. The following subsections detail the specific information for each instrumentation and sensor data type.

B. Inertial Measurement Units

Three IMUs were available for usage during various portions of the SR-1 flight test. These three devices are identified in Table 1 as Affordable Vehicle Avionics (AVA) [5], X-IO Next Generation IMU (NGIMU) [6], and Memsense H3-IMU [7]. Two of the devices, AVA and NGIMU, were integrated avionics components of the ADEPT SR-1 vehicle. The H3 IMU was the onboard IMU for the sounding rocket and is only relevant for ADEPT SR-1 reconstruction to the point of vehicle separation.

The AVA and NGIMU units were integrated in the ADEPT SR-1 vehicle as redundant IMU data sources for risk reduction purposes. Both units also provided independent magnetometer data measurements. However these were not used for reconstruction purposes. The AVA device also handled processing of the onboard GPS data. Each device stored data to internal memory for retrieval post flight. Since no data was telemetered, recovery of the flight vehicle and successful transfer of the collected data were critical for mission success. During the launch portion of the flight, both AVA and NGIMU were expected to saturate the X-axis gyroscope channel. This was due to the high roll rate experienced during the spin stabilized sounding rocket ascent.

The H3 IMU was an external data source available to the reconstruction process and was integrated with the sounding rocket launch vehicle. This unit provided ADEPT SR-1 relevant data from launch to vehicle separation. The H3 IMU was a critical data source for establishing the initial conditions of the ADEPT SR-1 vehicle at separation. During the spin stabilized portion of the ascent, the H3 IMU was the only device with an X-axis gyroscope capable of accurately measuring the angular rate of the vehicle. Table 2 details the specifications of the various IMUs. Uncertainties for these devices were determined via a combination of unit calibration and reference documentation.

Table 2 ADEPT SR-1 IMU Parameters.

IMU	Vehicle	Accelerometer Limits	Gyroscope Limits	Sample Rate
		$\pm g$	$\pm ^\circ/s$	Hz
AVA	ADEPT	18	450	100
NGIMU	ADEPT	16	2000	400
H3	Sounding Rocket	20	3000	800

C. Onboard Sensor Calibration

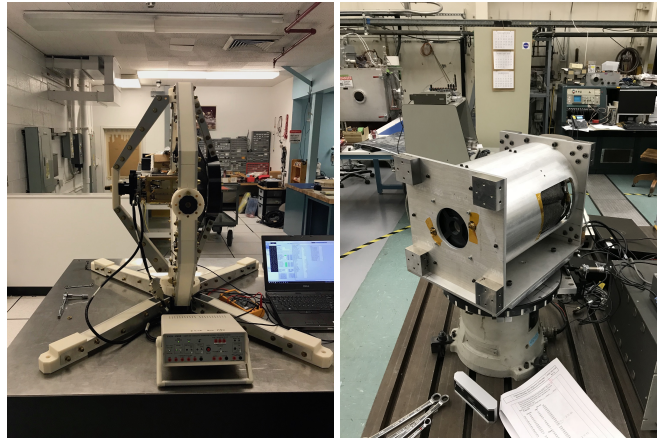
The ADEPT SR-1 IMUs, AVA, and NGIMU, record data from a suite of tri-axial sensors including an accelerometer, a gyroscope, and a magnetometer. At manufacturing, these sensors perform within a stated tolerance that addresses bias, scaling, alignment, repeatability, thermal sensitivity, etc. The ADEPT SR-1 team conducted a series of tests that calibrated each sensor independently to improve the overall accuracy of recorded data. The calculation of the calibration parameters input a data set of 500 consecutive points selected for minimum deviation. The calibration process yields parameters that resolve a bias, a scaling factor, and misalignment in each sensor. A bias is identified by nonzero values when no force is acting on the sensor. A scale factor captures nonlinearities between the output voltage of the sensor and the physical activity it measures. Bias and scale factor are each captured by three unknowns. Misalignment is an error between the sensor axes and the platform axes and is defined by six angles. These twelve parameters are solved by a least squares approach. The solution is used to create the components of rotation matrix T, the scale factor matrix K, and a bias vector. When applied to raw data, the calibration parameters when applied to raw data produce calibrated readings. These equations are shown in Equation 1 and Equation 2. Note, the tests described below discuss the collection of calibration enabling data and were performed with the IMUs mounted in the ADEPT SR-1 vehicle. This eliminates error and uncertainty associated with board misalignment; however, misalignment between the IMU sensors and the board must still be considered.

$$T = \begin{pmatrix} 1 & -a_{yz} & a_{zy} \\ a_{xz} & 1 & -a_{zx} \\ -a_{xy} & a_{yz} & 1 \end{pmatrix} \quad (1)$$

$$\mathbf{K}_a = \text{diag}(k_{x_a}, k_{y_a}, k_{z_a}) \quad (2)$$

The accelerometer calibration test was conducted on a flat table with SR-1 placed in a fixture to allow for rapid and precise rotation. The calibration process requires both positive and negative measurements from each accelerometer axis. To accurately define the axes, inclinometer readings were taken at several points on the electronics chassis. Data for calibration was recorded when SR-1 was within 0.1° of perpendicular to the table. The fixture used to support the flight vehicle for calibration is shown in Fig. 2. The specific value of gravity associated with the GPS coordinates of the test location was used as truth.

The gyroscope test was performed on a spin table. ADEPT SR-1 was placed in a fixture securing it during the rotations. The gyroscope calibration exercises both the positive and negative directions of the instrument and was excited to $\pm 120^\circ/\text{s}$, $\pm 240^\circ/\text{s}$, and $\pm 360^\circ/\text{s}$ states. An optical spin rate tracker was used to record the truth-value at each rate for each ADEPT SR-1 axis. Figure 2 shows the setup for testing the ADEPT SR-1 Y axis gyroscope. The rotation about Y-axis excited the X-axis gyro in the uncalibrated data. This was due to misalignment of the sensor. After calibration, these errors were corrected and the X-axis records the expected $0^\circ/\text{s}$.



(a) Accelerometer Calibration Fixture. (b) Gyroscope Calibration Table.

Fig. 2 IMU Calibration Devices.

The magnetometer calibration test requires a magnetically quiet area so as to not interfere with the instruments. The compass rose at Moffett Field, originally used to calibrate aircraft magnetometers was selected for this purpose. Using an independent magnetometer, magnetic north was identified and the magnetic field measured. The vehicle was placed into twenty four unique attitudes through X, Y, and Z rotations. This provided enough data to successfully complete calibration on the tri-axial suite of sensors.

Calibration of the H3 IMU was completed by the launch provider.

D. Global Positioning System

The only onboard GPS product expected was provided by the AVA sensor package. This device was a GPS receiver integrated with the AVA sensor suite, with a dedicated patch antenna. The unit was expected to deliver position, altitude, and associated uncertainties. However, it was discovered post flight that the onboard GPS unit was not able to establish a viable GPS solution after leaving the launch pad. Post flight investigation has suggested the high roll rate of the vehicle and the GPS unit software settings and thresholds may be the cause of lost data.

Post flight, it was discovered that a secondary payload on the sounding rocket contained a pair of GPS receivers. This payload, the Autonomous Flight Termination Unit (AFTU), provided position and velocity data and was used during the

reconstruction process. This GPS data provided numerous position and velocity measurements during the ascent phase of flight. Figure 3 contains a time versus altitude plot of the GPS data used in the ADEPT SR-1 reconstruction process.

E. Tracking Radar

Radar tracking of the ADEPT SR-1 flight vehicle was accomplished via an onboard C-band transponder. The transponder installed to allow tracking radars at the White Sands Missile Range to track the vehicle from launch to impact. Preflight coordination with the range was completed, and three distinct radar tracks were expected to be provided in the form of slant range, elevation, azimuth, and uncertainty values. However, the tracking radar data received by the ADEPT SR-1 team was limited to a post apogee period of time due to a misunderstanding with the White Sands Missile Range. This data was also provided in a latitude, longitude, and altitude format with no uncertainty values. These two deviations from the expected data directly impacted the ability to reconstruct the ADEPT SR-1 flight vehicle trajectory. Figure 3 is a graphical representation of the post apogee altitude information as a function of launch time obtained from the range.

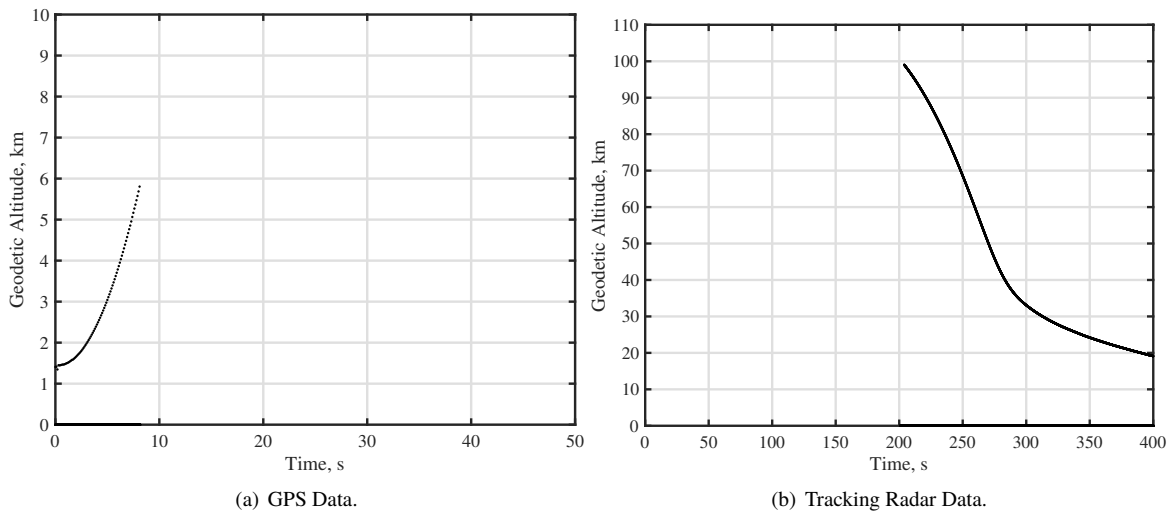


Fig. 3 Instrumentation & Sensor Data Sources.

F. Atmosphere Reconstruction

There were no in-situ sensors to take atmospheric measurements on-board ADEPT SR-1 or the launch vehicle; however, atmosphere-relative quantities like Mach number, angle of attack, and dynamic pressure were desired during the post-flight reconstruction. Thus, ADEPT SR-1 used a collection of launch services provided atmospheric measurements and weather model data to aggregate launch day atmospheric properties similar to other sounding rocket based tests in the recent past [8]. The data sources are summarized in Table 3.

Table 3 Atmospheric Datasets for ADEPT SR-1.

Dataset	Description
Balloonsonde	GPS receiver attached to weather balloon to take upper and lower altitude wind speed, pressure, and temperature measurements
GEOS-5 Analysis	Atmospheric model data reanalyzed with Earth-based observations
1976 US Standard Atmosphere	Pressure, temperature, and density at altitudes above GEOS-5 model data

The launch provider took several upper altitude and lower altitude atmospheric measurements before and after the

launch using weather balloons. The primary goal of these measurements was to provide wind speed measurements near the launch site that would influence the azimuth of the launch vehicle. The last minute adjustment of the launch vehicle azimuth to maintain the same landing site location is common practice for sounding rockets and is called wind weighting. However, these measurements are not designed for scientific assessment of the atmospheric profile during the launch trajectory, and the altitude of the measurements is capped by the capability of the weather balloon. For ADEPT SR-1, the highest altitude reached by these balloons was approximately 15 km geodetic altitude. The upper altitude balloons were 600 gram Hwoyee weather balloons, and the lower altitude balloons were 100 gram models of the same brand. A rise rate of roughly 5 m/s was targeted. The 600g Hwoyee balloon was paired with Ublox GPS breakout instrument, pressure sensors, and K-type thermocouple, while the low altitude weather balloon did not have pressure and temperature sensors but used an Adafruit breakout.

Above 15 km altitude, data from the Global Modeling and Assimilation Ocean (GMAO) at Goddard Space Flight Center (GSFC) were used to provide temperature, pressure, density, and wind speed information. GMAO creates predictions of Earth atmospheric properties daily at increments of 3 hours[9]. These predictions, known as GEOS-5, are then reanalyzed after the prediction time has passed with local observations to recompute the atmospheric state. These observations include radiosonde data from the National Weather Service, ground station measurements, radar wind sensors, and maritime data. Although GEOS-5 is not an in-situ weather measurement, the reanalysis data benefits from some in-situ measurements to improve the atmospheric estimate. GEOS-5 data is computed at a grid that is 0.5 deg in latitude and 0.625 deg in longitude. ADEPT SR-1 trajectory covered a large swath of latitude and longitude and so two grid points closest to the launch and landing sites respectively were used. Additionally, the GEOS-5 reanalysis data was available for 12:00 and 15:00 UTC, while the launch took place close to 13:30 UTC. So reanalysis data from both time points were used. Post-flight, GMAO provided data to quantify GEOS-5 uncertainties at the White Sands Missile Range region based on comparison with historical meteorological rocket data [9–12].

The GEOS-5 predictions are applicable to approximately 65 km geodetic altitude, which is above the scientific region on interest for ADEPT SR-1. However the vehicle trajectory was predicted to reach 115 km altitude. Therefore to ease the estimation of atmospheric quantities, the atmospheric reconstruction was extended to 125 km. The authors found no high quality measurements or models of atmospheric measurements at White Sands Missile Range that adequately captured local weather phenomenon. Thus, the 1976 US Standard Atmosphere data [13] was used to extend pressure, temperature, and density measurements above the GEOS-5 model height, and wind speeds were assumed to be zero. Figures 4- 6 summarize the various datasets used for ADEPT SR-1 atmospheric reconstruction and also show

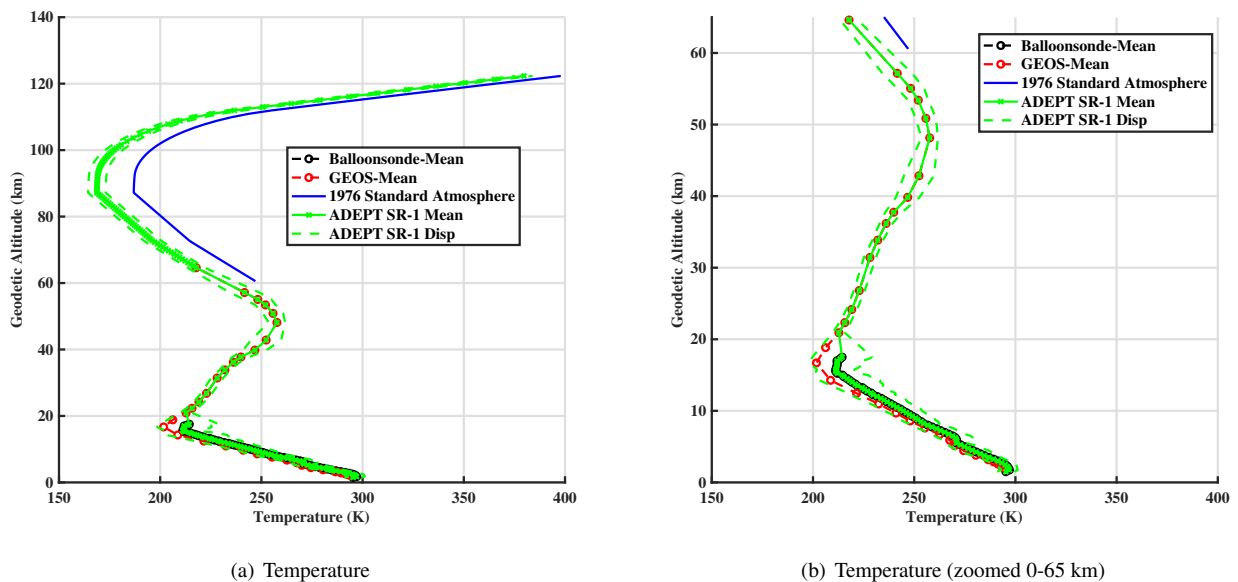


Fig. 4 ADEPT SR-1 Temperature reconstruction and the various datasets used during the process.

the final ADEPT SR-1 reconstructed atmosphere and uncertainties. In order to combine the various data sources, the

mean of each data source was taken at each altitude level. For the balloonsonde wind data, a moving average filter was also applied to cut-off high frequency noise and yield wind speeds that vary on the scale of hundreds of meters. From the ground to 15 km altitude, the temperature from the mean balloonsonde data was assumed to be the temperature along the flight path of the ADEPT SR-1. Figure 4 shows that there was a discrepancy between the GEOS-5 mean and balloonsonde mean, but since the balloonsonde data were actual measurements taken at locations flown by the ADEPT SR-1 spacecraft, they were taken as reconstructed values. From 15 km to 65 km, the mean GEOS-5 temperature profile was used. Finally, from 65 km and higher, the temperature profile from the 1976 US Standard atmosphere was used along with an adjustment that made the standard atmosphere-based profile equal to the GEOS-5 highest altitude temperature. Based on this ADEPT SR-1 temperature profile, pressure and density were calculated using the hydrostatic equation and perfect gas law. Finally, the wind profiles were also combined similar to the temperature profile with the additional assumption that wind speeds above 65 km were assumed to be zero. Note that RRA is the range reference atmospheric wind speed in September at the White Sands Missile Range and is provided for reference only.

The uncertainties for the region with only GEOS-5 data were based on comparing past predictions with historical meteorological rocket measurements at White Sands Missile Range. The uncertainties in temperate, density, and wind speeds were estimated. Uncertainties in pressure could not be computed since the GEOS-5 model makes predictions at constant pressure levels meaning pressure is the independent variable in the process. For the region below 15 km, the uncertainties for ADEPT SR-1, each individual profile from the balloonsodes and GEOS-5 predictions were compared with the ADEPT SR-1 mean estimate and the sample standard deviation of this difference was estimated as the uncertainties. In the region where standard atmosphere was used, the percentage uncertainty of the last GEOS-5 data point was used as the uncertainty for the region above 65 km.

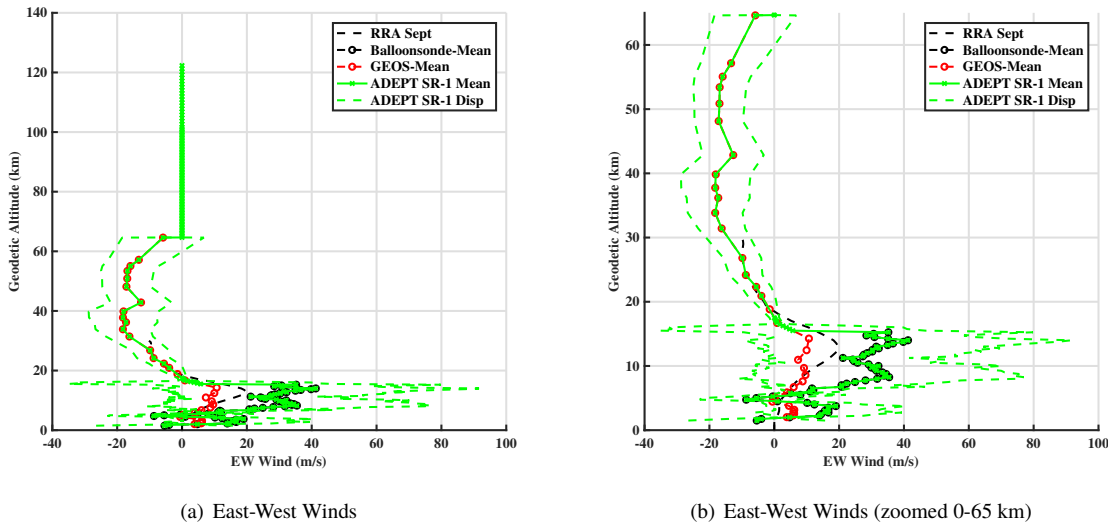


Fig. 5 ADEPT SR-1 East-West Wind reconstruction and the various datasets used during the process.

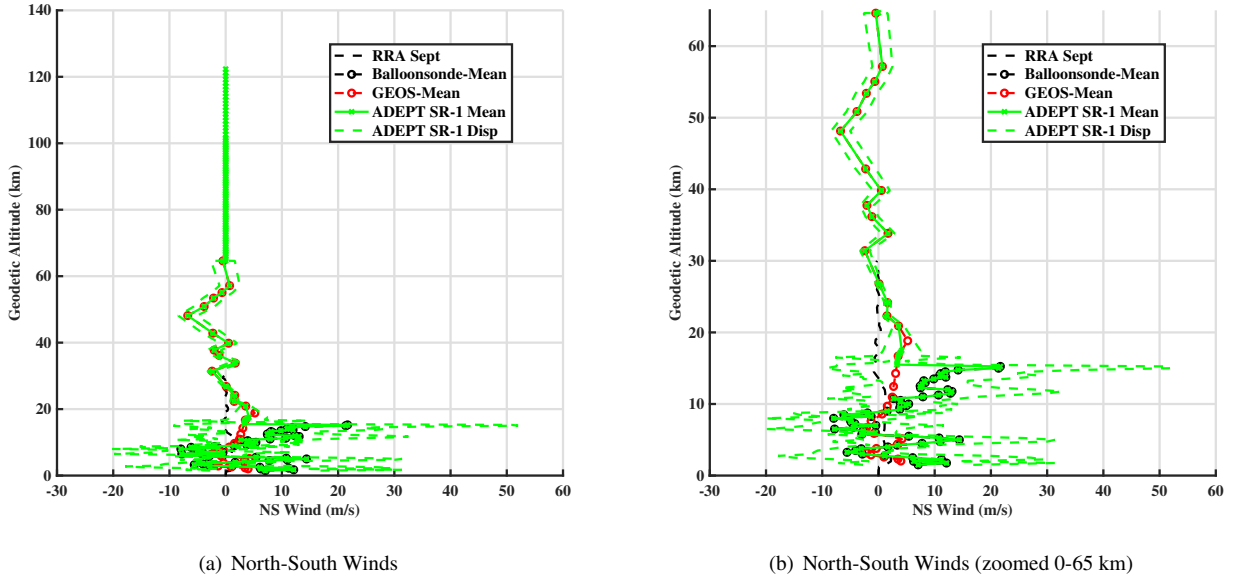


Fig. 6 ADEPT SR-1 North-South Wind reconstruction and the various datasets used during the process.

IV. SR-1 Data Analysis

A. Trajectory Reconstruction

The SR-1 flight vehicle reconstruction was performed utilizing the NewSTEP methodologies described previously. Various sensor suite combinations were explored during the reconstruction process, with the final results described in this section. The data products and sensors used for this process included the AVA IMU accelerations and angular rates, H3 X-axis angular rates, and radar and GPS data provided by external sources. The data products used in the final reconstruction were not the preflight sensor suite but was instead the logical solution matrix for the data received. Table 4 contains the matrix of sensors used in the following reconstruction results.

The uncertainties used during the reconstruction process were determined through a combination of preflight testing, sensor provided uncertainties, and best practices. The IMU uncertainty values were determined via a combination preflight calibration and testing or manufacturer specifications where applicable. The GPS units utilized for reconstruction provided estimated position and velocity uncertainties that were used for the reconstruction process. The radar data was the singular data source for which no native uncertainties were provided. The uncertainty values applied for the radar data was solely based upon prior experience with similar radar data sources and past experience with this flight testing range.

Table 4 Reconstruction Data Sources.

Sensor	Valid Use Times <i>sec</i>	Measurement Type	Source
AVA IMU	0-57	[X Y Z]Accelerations & [Y Z] Angular Rates	Onboard
H3 IMU	0-57	[X] Angular Rates	Sounding Rocket
AVA IMU	57-400	[X Y Z]Accelerations & [X Y Z] Angular Rates	Onboard
AFTU A GPS	0-8.3	Position & Velocity	Secondary Payload
AFTU B GPS	0-8.2	Position & Velocity	Secondary Payload
Tracking Radar	203.9-400	Position	Offboard

The final reconstruction was initialized from the launch pad and terminated at 400 seconds into the flight. At

Table 5 Trajectory Conditions at Key Test Events.

Event	Time from Launch <i>sec</i>	Altitude <i>m</i>	Mach	Dynamic Pressure <i>Pa</i>	Angle of Attack <i>deg</i>
ADEPT SR-1 Separation	96.31	93240	2.2267	0.1825	170.7872
ADEPT SR-1 Deploy	134.7	107760	0.8429	0.0016	-171.7977
Apogee	156.18	109930	0.4421	0.00030829	99.6279
ADEPT SR-1 Re-entry	229	84945	2.655	1.3248	15.8879
Peak Mach	254.37	64602	3.0954	66.483	-2.473
Peak Dynamic Pressure	281.9	40871	2.0536	818.4003	-0.493
Mach 0.8	306.63	31454	0.8	473.9746	-10.9537

approximately 400 seconds into the trajectory, the body rates on the vehicle exceeded the capabilities of the onboard IMUs, and IMU based reconstruction was no longer possible. Radar tracking continued after 400 seconds, and the approximate impact time of the vehicle was determined to be 857 seconds after launch.

The IMU sensor combination was established after data quality issues were discovered with the NGIMU unit onboard the vehicle. The onboard AVA IMU was utilized for acceleration and angular rate information from the launch pad to 400 seconds. However, during the first 57 seconds of the flight, the X-axis gyroscope channel from AVA was replaced with the X-axis gyroscope data from the H3 IMU. During this period the sounding rocket was aerodynamically spun to a roll rate higher than the capabilities of the AVA IMU. However, the H3 IMU sensor performance was capable of continuous operation during this period the the flight. As a consequence, from launch until de-spin the H3 IMU data was substituted in the X-axis angular rates for reconstruction purposes, approximately from launch to 57 seconds.

The launch and deployment of the ADEPT SR-1 from the launch vehicle was in-family with pre-flight predictions. The altitude at separation was approximately 107 km at with a vehicle roll rate of approximately 43°/s. The vehicle roll rate increased after re-entry and reached values greater than 300°/s prior to IMU saturation at 400 seconds. The angle of attack of the vehicle and sideslip of the vehicle remained below 20° during the peak Mach number and Mach 0.8 phase of flight, a key area of interest for the experiment.

The results presented in this paper are focused on the post ADEPT SR-1 separation portion of flight; key events during this portion of flight can be found in Table 5. Figure 7 through Fig.11 detail selected reconstruction results during the flight test from launch vehicle separation to IMU saturation at 400 seconds. Additional information regarding the flight vehicle performance and pre-flight predictions can be found in references [4], [14], and [15].

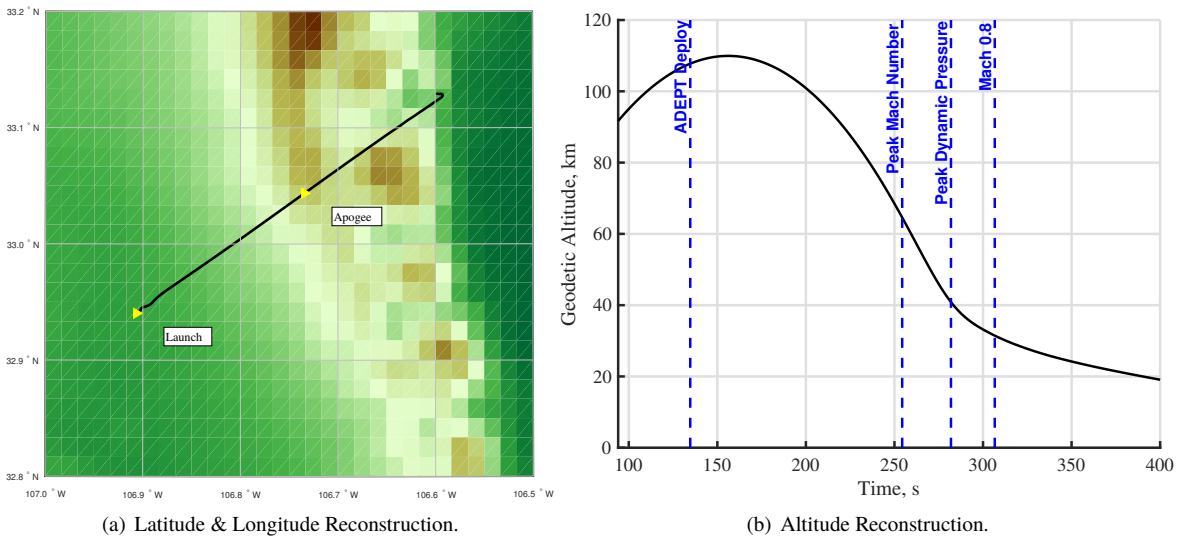


Fig. 7 Position and Altitude Reconstruction.

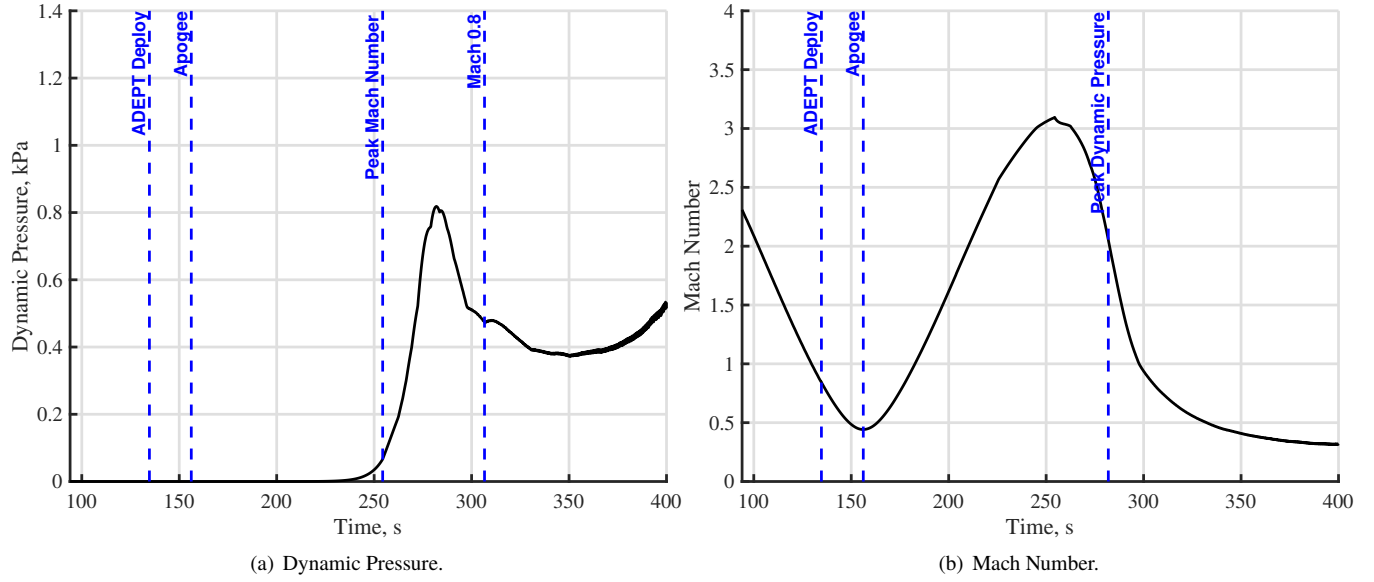


Fig. 8 ADEPT SR-1 Dynamic Pressure and Mach Number Reconstruction.

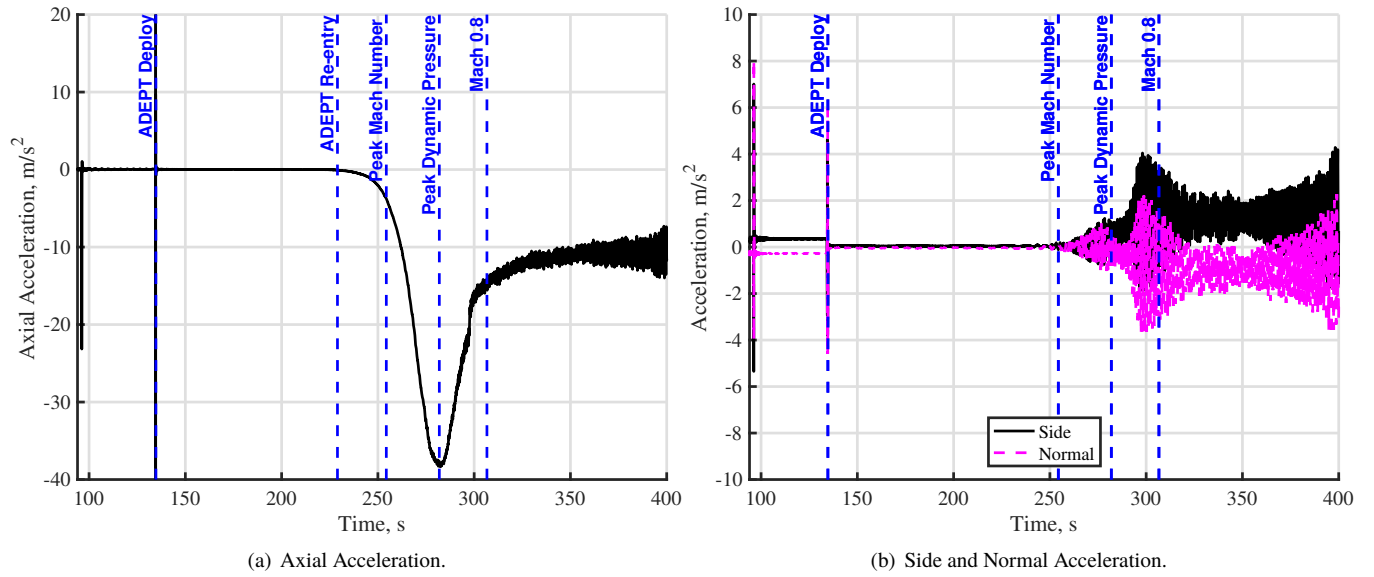


Fig. 9 ADEPT SR-1 Accelerations.

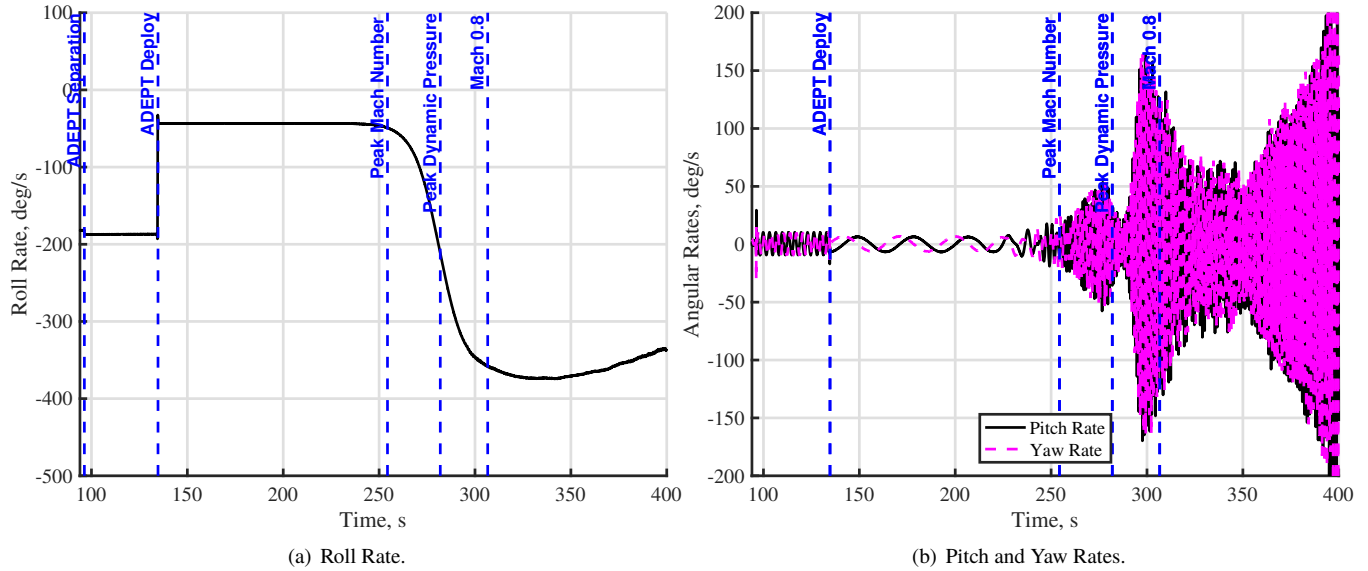


Fig. 10 ADEPT SR-1 Angular Rates.

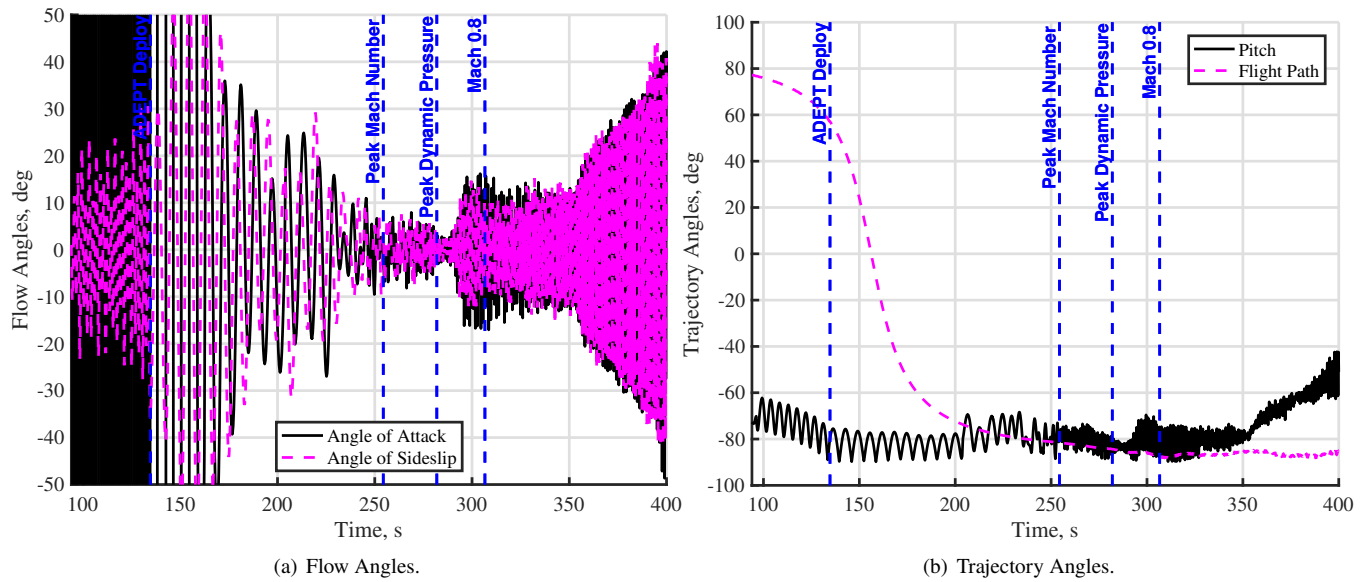


Fig. 11 ADEPT SR-1 Attitude Angles.

V. Conclusions

The successful launch and recovery of the ADEPT SR-1 flight vehicle provided the data products necessary for flight reconstruction of the performance history and aerodynamic components. The launch occurred on 12 September 2018, and the total flight time was approximately 857 seconds. 400 seconds of flight data were reconstructed, of which 304 seconds were of the ADEPT SR-1 vehicle in free flight. The vehicle was delivered within the nominal flight envelope by the launch provider and achieved a maximum Mach number and dynamic pressure of 3.09 and 818.4 Pa respectively.

Acknowledgments

The authors would like to thank Allen Minor of UP Aerospace and Erik Magnuson from NASA Kennedy Space Center for providing various ADEPT SR-1 datasets that were not part of the on-board measurements. Additionally, the

authors very much appreciate the GEOS-5 uncertainty analysis work done by Lawrence Coy of NASA Goddard Space Flight Center on a short time frame.

References

- [1] Karlgaard, C. D., Tartabini, P. V., Blanchard, R. C., Kirsch, M., and Toniolo, M. D., “Hyper-X Post-Flight Trajectory Reconstruction,” *Journal of Spacecraft and Rockets*, Vol. 43, No. 1, 2006, pp. 105–115.
- [2] Karlgaard, C. D., Tartabini, P. V., Martin, J. G., Blanchard, R. C., Kirsch, M., Toniolo, M. D., and N., T. M., “Statistical Estimation Methods for Trajectory Reconstruction: Application to Hyper-X,” Tech. rep., NASA TM-2009-215792, August 2009.
- [3] Striepe, S., Powell, R., Desai, P., Queen, E., Way, D., Prince, J., Cianciolo, A., Davis, J., Litton, D., Maddock, R., Shidner, J., Winski, R., O’Keefe, S., Bowes, A., Aguirre, J., Garrison, C., Hoffman, J., Olds, A., Dutta, S., Zumwalt, C., White, J., Brauer, G., Marsh, S., and Engel, M., *Program To Optimize Simulated Trajectories II (POST2), Vol. II: Utilization Manual*, Version 3.0.NESC, 2015.
- [4] Dutta, S., and Green, J., “Flight Mechanics Modeling and Post-Flight Analysis of ADEPT SR-1,” *AIAA SciTech 2019*, San Diego, CA, 2019.
- [5] Cockrell, J., “Affordable Vehicle Avionics (AVA),” , 2016. URL <https://ntrs.nasa.gov/archive/nasa/casi.ntrs.nasa.gov/20160008701.pdf>.
- [6] *NGIMU User Manual*, 1st ed., 2017. URL <http://x-io.co.uk/downloads/NGIMU-User-Manual-v1.3.pdf>.
- [7] *H3 IMU Product Specification User’s Guide*, psd 1001 rev b ed., 2010.
- [8] O’Farrell, C., Karlgaard, C., Dutta, S., Queen, E., Ivanov, M., and Clark, I., “Overview and Reconstruction of the ASPIRE Project’s SR01 Supersonic Parachute Test,” *IEEE Paper No. IEEE Aerospace Conference*, Big Sky, MT, 2018.
- [9] Modeling, G., and (2015), A. O. G., “MERRA-2 Specific Dataset 10.5067/6EGRBNEBMYIS,” , 2015.
- [10] Gelaro, R., McCarty, W., Suarez, M. J., Todling, R., Molod, A., Takacs, L., Randles, C. A., Darmenov, A., Bosilovich, M. G., Reichle, R., Wargan, K., Coy, L., Cullather, R., Draper, C., Akella, S., Buchard, V., Conaty, A., da Silva, A. M., Gu, W., Kim, G.-K., Koster, R., Lucchesi, R., Merkova, D., Nielsen, J. E., Partyka, G., Pawson, S., Putman, W., Rienecker, M., Schubert, S. D., Sienkiewicz, M., and Zhao, B., “The Modern-Era Retrospective Analysis for Research and Applications, Version 2 (MERRA-2),” *Journal of Climate*, Vol. 30, No. 14, 2017, pp. 5419–5454. doi:10.1175/JCLI-D-16-0758.1, URL <https://doi.org/10.1175/JCLI-D-16-0758.1>.
- [11] Randel, W., M.-L., C., and C., M., “Information about the SPARC (Stratosphere-troposphere Processes and their Role in Climate) Rocket Data Set (including the White Sands rockets),” , 2002.
- [12] Fujiwara, M., Wright, J. S., Manney, G. L., Gray, L. J., Anstey, J., Birner, T., Davis, S., Gerber, E. P., Harvey, V. L., Hegglin, M. I., Homeyer, C. R., Knox, J., Kruger, K., Lambert, A., Long, C. S., Martineau, P., Molod, A., Monge-Sanz, B. M., Santee, M. L., Tegtmeier, S., Chabrillat, S., Tan, D. G. H., Jackson, D. R., Polavarapu, S., Compo, G. P., Dragani, R., Ebisuzaki, W., Harada, Y., Kobayashi, C., McCarty, W., Onogi, K., Pawson, S., Simmons, A., Wargan, K., Whitaker, J. S., and Zou, C.-Z., “Introduction to the SPARC Reanalysis Intercomparison Project (S-RIP) and overview of the reanalysis systems,” *Atmospheric Chemistry and Physics*, 2017, pp. 1417–1452.
- [13] “U.S. Standard Atmosphere, 1976,” , 1976.
- [14] Korzun, A., Dutta, S., McDaniel, R., Karlgaard, C., and Tynis, J., “Aerodynamics for the ADEPT SR-1 Flight Experiment,” *AIAA SciTech 2019*, San Diego, CA, 2019.
- [15] Cassell, A., Wercinski, P., Smith, B., Yount, B., Ghassemieh, S., Nishioka, O., Kruger, C., C., B., Makina, A., Wu, S., Mai, N., McDaniel, R., Guarneros-Luna, A., Williams, J., Hoang, D., Rowan, R., Dutta, S., Korzun, A., Cruz, J., Green, J., Tynis, J., and Karlgaard, C., “ADEPT Sounding Rocket One Flight Test Overview,” *AIAA SciTech 2019*, San Diego, CA, 2019.